Diazonium-based impedimetric aptasensor for the rapid label-free detection of Salmonella typhimurium in food sample

Zahra Bagheryan, Jahan-Bakhsh Raoof, Mohsen Golabi, Anthony Turner and Valerio Beni

Original Publication:

Zahra Bagheryan, Jahan-Bakhsh Raoof, Mohsen Golabi, Anthony Turner and Valerio Beni, Diazonium-based impedimetric aptasensor for the rapid label-free detection of Salmonella typhimurium in food sample, 2016, Biosensors & bioelectronics, (80), 566-573.
http://dx.doi.org/10.1016/j.bios.2016.02.024

Diazonium-based impedimetric aptasensor for the rapid label-free detection of *Salmonella Typhimurium* in food sample

Zahra Bagheryan[1, 2], Jahan-Bakhsh Raoof[2], Mohsen Golabi[1], Anthony P.F. Turner[1], Valerio Beni[1a]*

[1]Biosensors and Bioelectronics Centre, Department of Physics, Chemistry and Biology (IFM), Linkoping University, 58183, Linkoping (Sweden)

[2]Eletroanalytical Chemistry Research Laboratory, Department of Analytical Chemistry, Faculty of Chemistry, University of Mazandaran, Babolsar, Iran

Corresponding author:

Dr. Valerio Beni Ph.D.

e-mail: valerio.beni@acreo.se

Current affiliation:

[a]ACREO SWEDISH ICT AB, Box 787, SE-601 17 Norrköping, Sweden

A B S T R A C T

Fast and accurate detection of microorganisms is of key importance in clinical analysis and in food and water quality monitoring. *S. typhimurium* is responsible for about a third of all cases of foodborne diseases and consequently, its fast detection is of great importance for ensuring the safety of foodstuffs.

We report the development of a label-free impedimetric aptamer-based biosensor for *S. typhimurium* detection. The aptamer biosensor was fabricated by grafting a diazonium-supporting layer onto screen-printed carbon electrodes (SPEs), via electrochemical or chemical approaches, followed by chemical immobilisation of aminated-aptamer. FTIR-ATR, contact angle and electrochemical measurements were used to monitor the fabrication process. Results showed that electrochemical immobilisation of the diazonium-grafting layer allowed the formation of a denser aptamer layer, which resulted in higher sensitivity. The developed aptamer-biosensor responded linearly, on a logarithm scale, over the concentration range 1×10^1 to 1×10^8 CFU mL^{-1}, with a limit of quantification (LOQ) of 1×10^1 CFU mL^{-1} and a limit of detection (LOD) of 6 CFU mL^{-1}. Selectivity studies showed that the aptamer biosensor could discriminate *S. typhimurium* from 6 other model bacteria strains. Finally, recovery studies demonstrated its suitability for the detection of *S. typhimurium* in spiked (1×10^2, 1×10^4 and 1×10^6 CFU mL^{-1}) apple juice samples.

Keywords:

Diazonium grafting, aptamer, *S. typhimurium*, label-free detection, electrochemical impedance spectroscopy, food analysis

1. Introduction

Salmonella Typhimurium (S. Typhimurium), the second most common serotype (after *Salmonella enteritidis*) found in humans, is responsible, worldwide, for about a third of all cases of foodborne diseases (Gupta et al. 2003). Salmonellosis is an increasingly important health concern and is usually associated with the consumption of *Salmonella*-contaminated foods, mainly of animal origin, including beef (Wells et al. 2001), pork (Malorny and Hoorfar 2005), poultry (Carli et al. 2001) and turkeys (Nayak et al. 2003). However, non-animal products, such as fresh vegetables and fruits, fruit juices and spices, have also been associated with infections. Fruit juices are becoming increasingly relevant vehicles for Salmonella infection (Jain et al. 2009; Sivapalasingam et al. 2004; Vojdani et al. 2008).

Currently, the detection of *Salmonella* in food still relies on culture-based approaches or on the combination of these with biochemical (immuno) assays. Despite being very accurate and having the ability discriminate between live and dead cells, these assays are time-consuming, tedious, impractical (Lazcka et al. 2007) and, more importantly, are not suitable for on-site and real-time applications (June et al. 1995).

Recently, DNA microarrays (Gardner et al. 2010) have been shown to offer new opportunities for pathogen detection in a multiplex format at reasonable cost and speed (2–3 h to get results). Real time PCR (RT-PCR) has consequently, rapidly become a common analytical techniques for pathogen detection (Jain et al. 2009; Postollec et al. 2011). Nevertheless, PCR based analytical approaches are still far from being applicable to real-time or on-site analysis, since they still require well-equipped laboratories.

Biosensors have been extensively explored for pathogen detection with the aim of developing new tools for fast, low cost, real-time and on-site detection or screening. The simplest format for microbial monitoring is based on the detection of generic biomarkers, shared by most of the microorganism, such as ATP. ATP bioluminescence assays have been used, for the last three decades, for the rapid monitoring of surface microbial loading in the food industry and hospitals (Driscoll et al. 2007).

Assays based on the affinity between a ligand (antibodies, bacteriophages or lectins) and receptors onto the microbial cell surface have also been widely investigated (Karmali 2009). Antibody-based immunosensors have been the most explored approach in the development of portable pathogen detection (Chung et al. 2014; Seymour et al. 2015). However, the limited stability of antibodies is a major drawback in their widespread utilisation.

Aptamers are short single-stranded oligonucleotides that can bind, with high affinity, to a wide range of targets (Jayasena 1999) and are usually selected through an *in vitro* process using an exponential enrichment process (SELEX) (Chiu and Huang 2009). They have been explored as possible replacements for antibodies in bioaffinity assays and their potential for delivering real-time detection of microbial cells, from a variety of samples types, has been demonstrated (Dwivedi et al. 2010; Hamula et al. 2011; Joshi et al. 2009; Kaerkkaeinen et al. 2011; Ozalp et al. 2013; Torres-Chavolla and Alocilja 2009a, b; Wu et al. 2012). Among the different transduction approaches used for aptasensing, electrochemistry is of particular significance because of its advantages, such as high sensitivity, selectivity, simple instrumentation and low endogenetic background (Labib et al. 2012; Zelada-Guillen et al. 2009).

Stable and controllable immobilisation of biorecognition elements onto transducing surfaces is of great importance in the development of electrochemical biosensors. Currently the most

commonly adopted approach takes advantage of the strong affinity between SH groups and gold surfaces to produce self-assembled monolayer (SAM)-based platforms (Brasil de Oliveira Marques et al. 2009; Peterlinz et al. 1997). SAMs have found widespread application, but still present significant limitations: the surface modification is time consuming and its stability can be affected by different factors such as electrical potentials (Lockett and Smith 2009), UV irradiation (Shewchuk and McDermott 2009) and high temperatures (Civit et al. 2010). Some of these limitations have been overcome by the use of diazonium chemistry (Belanger and Pinson 2011; Galli 1988), which offers several advantages in terms of speed, simplicity and stability (Civit et al. 2010; Torréns et al. 2015b). Diazonium-grafted surfaces have found widespread application in different areas such as sensors (Corgier et al. 2005b, 2007) and catalysis (Bourdillon et al. 1992b). Diazonium grafted layers have a long-term stability under atmospheric conditions (Allongue et al. 1997) and are minimally affected by ultrasound treatments (Adenier et al. 2006), high temperatures (Civit et al. 2010) and electric potentials (Haque and Kim 2011; Piper et al. 2011; Revenga-Parra et al. 2012). Diazonium molecules modified with various functional groups have been introduced onto electrodes for immobilisation of biomolecules such as enzymes (Bourdillon et al. 1992a; Liu et al. 2007; Polsky et al. 2007; Radi et al. 2006), proteins (Corgier et al. 2005a) and antibodies (Corgier et al. 2005a; Ho et al. 2010) for biosensing application. To the best of our knowledge, there are just a few reports on the use of this chemistry for immobilisation of DNA (Ruffien et al. 2003; Shabani et al. 2006; Torrens et al. 2015a; Torrens et al. 2015b) and these were only for hybidisation assays.

Herein, we report on the development of a label-free impedimetric biosensor for *Salmonella enterocs serover. Typhimurium* (*S. typhimurium)* detection. More specifically screen-printed electrodes (SPEs) were modified with diazonium salt through electrochemical and Zn-mediated

chemical grafting and the properties, of the fabricated aptasensors based on these were compared in terms of surface density of the aptamer layer and sensitivity. The analytical performances of the sensors were then further investigated and the detection of *S. typhimurium* in spiked apple juice sample was demonstrated.

The aptasensor developed via electrochemical grafting had higher sensitivity and responded linearly over the concentration range 1×10^1 to 1×10^8 CFU mL^{-1}. It also had high selectivity in the presence of other pathogens and was suitable for the detection of *S. typhimurium* in spiked apple juice samples.

2. EXPERIMENTAL

2.1. Reagents

All reagents were of analytical grade and used as received. N-ethyl-N'-(3-dimethylaminopropyl) carbodiimide hydrochloride (EDC), 4-aminbenzoic acid, tetrafluoroboric acid solution, zinc powder, sodium nitrite 99.5%, potassium ferricyanide (III) and potassium ferrocyanide (II), were purchased from Sigma–Aldrich (Sweden) .

All pathogenic strains used in this work were acquired from the Culture Collection (the three E. coli strains), University of Gothenburg, Sweden or donated from the Linköping University Hospital (*Salmonella typhimurium*, *Entrobacter aerogenes*, *Citrobacter freundii* and *Kelebsiella pneumonia*).

The aminated DNA aptamer against *Salmonella* was purchased from biomers.net (Germany). The sequence of the aptamer (N 45 in the original work), selected against S. typhimurium outer membrane proteins (OMPs), was obtained from the work of Joshi et al. (Joshi et al. 2009):

5'- NH_2- ttt ggt cct tgt ctt atg tcc aga atg cga gga aag tct ata gca gag gag atg tgt gaa ccg agt aaa ttt ctc cta ctg gga tag gtg gat tat-3'

2.2 Pathogen preparation:

The cultivation of *S. Typhimurium,* and of the other pathogenic strains used in this work, was performed in nutrient broth (NB) medium at 37° C by shaking at 170 rpm for 16 h. The cultures containing bacteria were centrifuged at 3 765 g for 5 min (25 °C) and washed with PBS (0.1 M, pH 7.4) three times. After washing, the pellet was suspended in 15 mL of PBS and used as the original *S. typhimurium* stock solution; all other concentrations were made by diluting this in PBS. The pathogen concentration in the stock solution was estimated by measuring the optical density at 600 nm. Correlation between optical density and bacterial concentration (CFU mL^{-1}) was determined, at the beginning of this work, by the standard plate count method for each bacterial strain.

2.3 Instrumentation

Voltammetric experiments were carried out using an Ivium Stat. XR electrochemical analyser coupled with dedicated software (Ivium, Eindhoven, Netherlands). The impedance spectra were recorded within the frequency range of 100 kHz to 0.05 Hz in 5 mM $K_3[Fe(CN)_6]/K_4[Fe(CN)_6]$ (1:1) mixture in 10 mM PBS (pH 7.4) at a bias potential of 0 mV vs OCP potential. The amplitude of the applied sine wave potential was 5 mV. The Nyquist plots obtained were fitted to an equivalent circuit to extract the value of charge-transfer resistance (R_{ct}). Chronocoulometry was used for the determination of aptamer surface coverage. The following parameters were used to perform the chronocoulometric measurements: pulse period= 500 ms, pulse width= 500 mV.

Screen-printed electrodes (SPEs) consisted of a carbon working electrode (4 mm in diameter); a carbon counter electrode and a silver pseudo-reference electrode printed onto a ceramic substrate; these were purchased from Dropsens, Spain (Manufacturer code DRP-110). All the experiments were carried out at room temperature (21°C). ATR-FTIR measurements were obtained using a PIKE MIRacle ATR accessory with a diamond prism in a Vertex 70 spectrometer (Bruker) using a DTGS detector at room temperature under continuous purging of N_2. IR spectra were obtained at 4 cm^{-1} resolution and 32 scans between 4000 and 800 cm^{-1}. The static water contact angles of the films were measured using the sessile drop technique with fresh Milli Q water (18.2 MΩ) with the aid of a CAM200 Optical Contact Angle Meter (KVS Instrument, Finland).

2.3 Synthesis of 4-Amino benzoic acid tetrafluoroborate (ACOOH)

4-Aminobenzoic acid tetrafluoroborate was synthesised by dissolving 1.16 gr (8.5 mmol) of 4-aminobenzoic acid in 9 ml of 50% w/w aqueous tetrafluoroboric acid solution. The solution was heated until the 4-aminbenzoic acid completely dissolved and was then cooled in an ice water bath. Following dissolution of the amine, a cold solution of 0.73 g (10.5 mmol) of sodium nitrite in 2 ml MilliQ water was added dropwise to the reaction mixture with stirring. The slurry was cooled in an ice bath to favor crystallisation. The resulting white solid was collected on a Buchner funnel, washed with ice water and cold ether, dried under vacuum and finally stored at –4 °C in the dark (Baranton and Bélanger 2005; Dunker et al. 1936; Polsky et al. 2008). The presence of the diazonium functional group in the synthesised compound was confirmed by IR spectra.

2.4 Modification of SPEs through electrochemical grafting and Zn-mediated grafting

Electrochemical grafting: The electrochemical grafting was performed using a solution of 5 mM of ACOOH in 0.5 M cold sulphuric acid. A drop of diazonium solution (50 µL) was placed onto the SPE and then 10 cyclic voltammograms were recorded over the range from 0 to -1 V at 0.2 V/s (Ho et al. 2010).

Zn-mediated grafting: To modify the electrodes through Zn-mediated chemical grafting, a mixture of 20 µL of 5 mM of ACOOH in 0.5 M sulphuric acid containing an excess of Zn powder was stirred for 5 min under a stream of N_2, added to the electrode surface and left to react for 5 min (Torréns et al. 2015b).

2.5 Preparation and characterisation of aptasensors:

Following modification with the diazonium-grafting layer the electrodes were sonicated in water for 1 min, in order to remove weakly bounded molecules, and dried under a stream of N_2. The carboxyl groups present in the grafted diazonium layer were activated with 4:1 molar ratio of EDC (200 mM): NHS (50 mM) in water for 30 min. After rinsing with water and draying under nitrogen stream, a drop of 4 µM aminated-DNA aptamer (in 10 mM PBS buffer pH 7.4) was placed on the activated surface for 1 h. The unreacted carboxylate groups were then deactivated with 1 mM ethanolamine (pH 8) for 30 min. Finally, the modified electrodes were washed in PBS solution for 30 min to remove unspecifically chemisorbed aptamers. The ability of the developed aptasensors to detect *S. typhimurium* was assessed by testing them with solution containing different concentrations of the bacterias. The overall process is summarised in Scheme 1.

2.7 Bacteria measurements

Detection of bacteria was performed accordingly to the following protocol: aptasensors were incubated for 30 min (Labib et al. 2012) in the 10 mM PBS buffer (pH 7.4) solution containing the bacteria or in the spiked apple juice sample; this step was performed by immersing the aptasensors in 10 mL of the tested solution. Following a 15 min wash in 10 mM PBS buffer (pH 7.4) electrodes were immersed in the 10 mM PBS buffer (pH 7.4) containing the 5 mM $K_3[Fe(CN)_6]/K_4[Fe(CN)_6]$ (1:1) mixture where EIS spectra were recorded accordingly to protocol described in section 2.3. A calibration curve was constructed by exposing the aptasensor to increasing concentrations, from 10^1 to 10^8 CFU mL $^{-1}$, of *S. typhimurium*. Each of the point in the calibration curve, selectivity curves and in the spiked sample analysis were the average of 3 measurements performed using 3 individual electrodes.

LOCATION OF SCHEME 1

3. RESULTS AND DISCUSSION

3.1. FTIR spectra

Diazonium salt was synthesised *ex-situ* according to the protocol described above (section 2.3) and characterised by FTIR-ATR (Supplementary material, Fig S1). As can be seen from Fig. S1, where the FTIR-ATR spectra of 4-aminbenzoic acid before and after diazonium formation are compared, a new band appeared after diazonium formation at about 2304 cm^{-1}. This new band has been previously associated with the (C-N=N) group in diazonium salt (Socrates 2001). A shift in the FTIR peak for carboxylic acid from 1656 cm^{-1} to 1718 cm^{-1} has also been recorded in the case of the diazonium salt; this shift can be the result of the electron acceptor properties of the newly formed diazo group.

234

235 3.2. Electrochemical characterisation of the aptasensor

236 Electrochemical impedance spectroscopy (EIS) measurements were used to characterise the
237 step-by-step assembly of the aptasensor. Fig. 1 shows the Nyquist plots obtained for a SPE (a),
238 ACOOH/SPE (b) and aptamer/ACOOH/SPE (c), via electrochemical (solid line) and Zn
239 mediated chemical grafting (dotted line). Measurements were performed using a 5.0 mM
240 $[Fe(CN)_6]^{3-/4-}$ couple (1:1) solution in 10 mM PBS (pH 7.4).

241

242 **LOCATION FIGURE 1**

243

244 As can be seen from Fig. 1, the impedance dramatically increased following ACOOH grafting,
245 regardless of which approach (electrochemical or Zn-mediated) was adopted for the surface
246 modification, indicating successful grafting of the ACOOH. Increases in R_{ct} were the result of
247 the formation of a highly packed negatively charged film on the electrodes surface that was
248 effectively blocking, via electrostatic repulsion, the diffusion of the $[Fe(CN)_6]^{3-/4-}$ couple to the
249 sensor surface. A higher blocking effect was achieved, as expected, for the electrochemical
250 grafting; this was probably due to the higher level of immobilisation or to the formation of
251 multilayers (Kariuki and McDermott 1999). The value of R_{ct} dramatically decreased after DNA
252 aptamer immobilisation (curves C of Fig. 1). This was the result of the lower density of negative
253 charges associated with: (i) the low density and the 3D structure of the bulky aptamer chain
254 (when compared to the ACOOH) and (ii) the partial neutralisation of the COOH originally on the
255 surface due to the blocking step with ethanolamine (Hayat et al. 2012; Hayat et al. 2011).
256 Modeling of the impedance data was realised according to the Randles circuit depicted in the

inset of Fig. 1. This is based on the charge transfer resistance (R_{ct}), the constant phase element (CPE), the solution resistance (R_s) and the Warburg impedance (W).

3.3. Contact angle measurement:

The success of the assembly was also confirmed by contact angle measurement. In order to record this, a drop (10 µl) of fresh Milli Q water (18.2 MΩ) was placed onto the unmodified and/or modified surfaces and five images were recorded using a CAM200 Optical Contact Angle Meter. Fig. S2 summarises the average of the contact angle values obtained. Contact angle decreased sequentially after diazonium salt and aptamer immobilisation, regardless of the grafting process adopted. The decrease in contact angle is due to the increased hydrophilicity of the surface due firstly to the introduction of the COOH group, and secondly to the immobilisation of the DNA aptamer.

3.4 Determination of aptamer surface density:

Aptamer surface coverage for the two constructed aptasensors (via electrochemical and Zn-mediated chemical grafting) was obtained using the well-established DNA/$[Ru(NH_3)_6]^{3+}$ interaction and chronocoulometric measurements (Wang et al. 2010; Yu et al. 2003). It is known that $[Ru(NH_3)_6]^{3+}$ binds to the anionic phosphate base of DNA in 1 to 3 ratio. Thereby calculation of surface DNA (Γ_{DNA}) coverage can be performed by determining the $[Ru(NH_3)_6]^{3+}$ entrapped in DNA layer (Γ_0). In Fig. 2 the typical chronocoulometric curves recorded during this evaluation are presented.

LOCATION FIGURE 2

Measurements were recorded at the aptamer modified electrodes in the absence and presence of 50 μM of $[Ru(NH3)_6]^{3+}$. Assuming that the double layer capacitance remains approximately constant, $nFA\Gamma_0$ (Eq. 1), the charge from the reduction of absorbed redox marker, can be measured by using the difference in intercepts:

$$Q = nFA\,\Gamma_0 \qquad \text{Eq. 1}$$

Where n is the number of electrons per molecule for reduction, F the Faraday constant (C/equiv), A the electrode area (cm^2) and Γ_0 is the surface excess of adsorbed redox marker.

The active areas of the electrodes were determined using the simplified Randles–Sevcik expression at 25 °C by carrying out cyclic voltammetry of 5 mM $[Fe(CN)_6]^{3-/4-}$ in 0.2 M KCl at different scan rates. The area for carbon screen-printed electrode was calculated to be 0.0028±0.00014 cm^2 (geometric surface area 0.00125 cm^2). As expected, the calculated active area is significantly larger than the geometrical one, due to the rough morphology of the electrode material.

The surface coverage of aptamer can be calculated from the integrated Cottrell expression at time=0 (Eq. 2) in the absence and presence of redox marker using the relationship:

$$\Gamma_{DNA} = \Gamma_0\,(z/m)\,N_A \qquad \text{Eq. 2}$$

Where Γ_{DNA} is aptamer surface density (molecule /cm^2), z is the charge of the redox molecule, m is the number of bases of aptamer (96) and N_A Avogadro's number.

Surface coverages of 6.25×10^{13} (molecule /cm^2) for the electrochemical grafting method and of 5.33×10^{12} (molecule /cm^2), for the Zn-mediated chemical grafting were obtained. As can be seen, the aptamer surface coverage was higher in the case of electrochemical grafting method. The surface coverage results obtained herein differed from those reported by Torrens et al.

(Torréns et al. 2015a); in our case the surface density was higher in the electrochemical approach that in the Zn-mediated method. These results could be due to the formation of a denser and more easily self-organised layer, due to the small sizes of the 4-amino benzoic acid tetrafluoroborate when compared to 5-bis(4-diazophenoxy)benzoic acid tetrafluoborate.

3.5 Electrochemical detection of *S. typhimurium:*

The *S. typhimurium* detection was performed by immersing the aptasensor in a solution of bacteria (in 10 mM PBS pH 7.4) for 30 min (Labib et al. 2012), followed by EIS measurements. To be sure that the PBS buffer did not have any effect on the impedimetric response of the aptasensor, the response obtained for the sensor as the function of the immersion time in pure (no bacteria) PBS was studied. This was performed by immersing the aptasensor in PBS solution, in the presence of the $[Fe(CN)_6]^{3/4}$ couple, and recording EIS measurements every 15 min. Fig. S3 shows that the R_{ct} was increasing over the first 30 min; this increase was probably due to the 3D reorganisation of the aptamer on the sensor surface. After this initial period of change, the R_{ct} became constant. To minimise this effect the aptasensors were pre-conditioned in PBS solution, for 30 min, prior to bacteria detection.

The analytical performances of the aptasensors prepared using the two grafting approaches, were compared by using them for the detection of two concentrations of *S. typhimurium* (1×10^2 and 1×10^8 CFU mL^{-1}). Fig 3A shows that the responses recorded from the electrochemically grafted aptasensor were consistently higher than those obtained by the chemical grafting. These results are most likely related to the higher surface density of the aptamer layer (see section 3.4).

LOCATION FIGURE 3

In the light of this result, full calibration, selectivity and recovery experiments were only performed using the aptasensor fabricated by the electrochemical grafting approach.

The aptasensors were calibrated using various concentrations of *S. typhimurium* (from 1×10^1 to 1×10^8 CFU mL^{-1}) and following the protocol described in Section 2.6. Capture of *S. typhimurium* onto the aptasensor surface resulted in an increase of the R_{ct}; this can be explained either by the physical blocking effect of the captured bacteria or by the electrostatic repulsion between the negatively charged bacterial cells and the $[Fe(CN)_6]^{3-/4-}$ redox probe. As it can be seen from Fig. 3B, R_{ct} values increased linearly with the logarithmic concentration of the bacteria in the range from 1×10^1 to 1×10^8 CFU mL^{-1}. The LOD (as 3 times the standard deviation of the blank, no pathogen, experiment) was determined to be 6 CFU mL^{-1}. It was also found that the aptasensor could be easily regenerated by dissociating the aptamers from the bacteria in 2 M NaCl for 30 min, as demonstrated by impedance and staining experiments (Fig S4).

Reproducibility of the aptasensor was calculated over the full range of concentration; this resulted in an average RSD of 15% (n=3 for each of the 8 concentrations used).

The ability of the aptasensor to distinguish between target bacteria and other bacteria strains was also investigated by EIS experiments. In this set of experiment solutions containing 10^6 CFU mL^{-1} of different bacteria were used. 10^6 CFU mL^{-1} was chosen because it has been demonstrate to provide relevant information on specific interaction between bacteria surfaces (Golabi et al., 2016).

LOCATION FIGURE 4

Fig. 4 shows that very small responses were recorded with the other investigated bacteria (three different kinds of *Escherichia coli (CCUG 3274, CCUG53375, and CCUG10979), Entrobacter aerogenes, Citrobacter freundii* and *Kelebsiella pneumonia*), thus indicating that the aptasensor is highly specific for *S. Typhimurium.*

3.6 Recovery studies and *Salmonella* determination in apple juice

To demonstrate the applicability of the proposed aptasensor to real samples analysis, recovery studies on spiked apple juice samples were performed. The responses of the aptasensor where then fitted to the calibration curve (Y=0.116X+0.0107) shown in Fig. 3B, in order to calculate the concentration of recovered *S. typhimurium* from the sample. Reproducibility of the detection was calculated for both spiked concentration (n=3); this resulted in an average RSD of 18.6%.

LOCATION FIGURE 5

Fig. 5 shows the response of the aptasensor in the absence and presence of different concentration of spiked bacteria in apple juice. The apple juice had no significant effect on the aptasensor response, while on addition of different concentration of *S. typhimurium*. (1×10^2, 1×10^4 and 1×10^6 CFU mL^{-1}) the R_{ct} increased significantly. As can be seen in the inset of Fig. 5, the aptasensor achieved good recovery illustrating its applicability for real sample analysis.

4. CONCLUSION

We report the development of a label-free, impedimetric biosensor for *S. typhimurium* detection. Two different approaches, based on electrochemical and Zn-mediated chemical grafting, have been explored and compared for the fabrication of an aptasensor, .

Electrochemical grafting of 4-amino benzoic acid tetrafluoroborate facilitated the formation of a denser (*ca.* 2 times) aptamer biorecognition layer. The electrochemically prepared aptasensor was more sensitive for detection at both low (1×10^2 CFU mL^{-1}) and high (1×10^8 CFU mL^{-1}) concentrations of *S. typhimurium*, compared to the Zn-mediated chemically grafted devices. The aptasensor responded linearly to the logarithm of the *S. typhimurium* concentration over the range 1×10^1 to 1×10^8 CFU mL^{-1} and was highly selective for *S. typhimurium* with a LOQ of 10^1 CFU mL^{-1} and a LOD of 6 CFU mL^{-1}. Finally, recovery experiments demonstrated that the sensor was suitable for the detection of three different concentrations of *S. typhimurium* (1×10^2, 1×10^4 and 1×10^6 CFU mL^{-1}) in apple juice. Comparison (Table 1S) of the performance of the reported aptasensor with those of relevant label-less electrochemical (impedimetric or potentiometric) aptasensors, indicates that the developed aptasensor has an LOD comparable to existing state of the art, but with a larger dynamic range. More significantly and more importantly and in contrast to previous work (Sheikhzadeh et al, 2016; Ma et al., 2014), the aptasensor worked in undiluted real sample.

5. ACKNOWLEDGMENT

ZB acknowledges the Ministry of Science Research and Technology of Iran (www.msrt.ir) to support her study visit at Linköping University. The authors acknowledge Vetenskapsrådet

(Pathoscreen project; Swedish Research Link; ref.-ID: D0675001) for supporting the development of the aptasensor and Dr. V. C. Ozalp for helping with the aptamer identification.

6. REFERENCE:

Adenier, A., Barré, N., Cabet-Deliry, E., Chaussé, A., Griveau, S., Mercier, F., Pinson, J., Vautrin-Ul, C., 2006. Surf. Sci. 600(21), 4801-4812.
Allongue, P., Delamar, M., Desbat, B., Fagebaume, O., Hitmi, R., Pinson, J., Savéant, J.-M., 1997. J. Am. Chem. Soc. 119(1), 201-207.
Baranton, S., Bélanger, D., 2005. J. Phys. Chem. B 109(51), 24401-24410.
Belanger, D., Pinson, J., 2011. Chem. Soc. Rev. 40(7), 3995-4048.
Bourdillon, C., Delamar, M., Demaille, C., Hitmi, R., Moiroux, J., Pinson, J., 1992a. J. Electroanal. Chem. 336(1-2), 113-123.
Bourdillon, C., Delamar, M., Demaille, C., Hitmi, R., Moiroux, J., Pinson, J., 1992b. J. Electroanal. Chem. 336(1), 113-123.
Brasil de Oliveira Marques, P.R., Lermo, A., Campoy, S., Yamanaka, H., Barbé, J., Alegret, S., Pividori, M.I., 2009. Anal. Chem. 81(4), 1332-1339.
Carli, K.T., Unal, C.B., Caner, V., Eyigor, A., 2001. J. Clin. Microbiol. 39(5), 1871-1876.
Chiu, T.-C., Huang, C.-C., 2009. Sensors 9(12), 10356.
Chung, B., Shin, G.W., Choi, W., Joo, J., Jeon, S., Jung, G.Y., 2014. Electrophoresis 35(23), 3283-3289.
Civit, L., Fragoso, A., O'Sullivan, C.K., 2010. Electrochem. Commun. 12(8), 1045-1048.
Corgier, B.P., Marquette, C.A., Blum, L.J., 2005a. J. Am. Chem. Soc. 127(51), 18328-18332.
Corgier, B.P., Marquette, C.A., Blum, L.J., 2005b. J. Am. Chem. Soc. 127(51), 18328-18332.
Corgier, B.P., Marquette, C.A., Blum, L.J., 2007. Biosens. Bioelectron. 22(7), 1522-1526.
Driscoll, M., Ramsay, C., Watkin, J., 2007. improved sensitivity method for rapid hygiene monitoring using atp bioluminescence. pp. 79-82.
Dunker, M.F.W., Starkey, E.B., Jenkins, G.L., 1936. J. Am. Chem. Soc. 58(11), 2308-2309.
Dwivedi, H.P., Smiley, R.D., Jaykus, L.-A., 2010. Appl. Microbiol. Biotechnol. 87(6), 2323-2334.
Galli, C., 1988. Chem. Rev. 88(5), 765-792.
Gardner, S., Jaing, C., McLoughlin, K., Slezak, T., 2010. BMC Genomics 11(1), 1-21.
Golabi, M., Turner APF., Jager EWH., 2016. Sensors and Actuators B 222, 839-848.
Gupta, A., Fontana, J., Crowe, C., Bolstorff, B., Stout, A., Duyne, S.V., Hoekstra, M.P., Whichard, J.M., Barrett, T.J., Group, t.N.A.R.M.S.P.W., 2003. J. Infect. Dis 188(11), 1707-1716.
Hamula, C.L.A., Zhang, H., Li, F., Wang, Z., Le, X.C., Li, X.-F., 2011. Trac.Trend. in Anal. Chem. 30(10), 1587-1597.
Haque, A.-M.J., Kim, K., 2011. Chem. Commun. 47(24), 6855-6857.
Hayat, A., Barthelmebs, L., Marty, J.-L., 2012. Sens. Actuators B: Chem. 171–172, 810-815.
Hayat, A., Barthelmebs, L., Sassolas, A., Marty, J.-L., 2011. Talanta 85(1), 513-518.

Ho, J.-a.A., Hsu, W.-L., Liao, W.-C., Chiu, J.-K., Chen, M.-L., Chang, H.-C., Li, C.-C., 2010. Biosens. Bioelectron. 26(3), 1021-1027.
Jain, S., Bidol, S.A., Austin, J.L., Berl, E., Elson, F., Williams, M.L., Deasy, M., Moll, M.E., Rea, V., Vojdani, J.D., Yu, P.A., Hoekstra, R.M., Braden, C.R., Lynch, M.F., 2009. Clin. Infect. Dis. 48(8), 1065-1071.
Jayasena, S.D., 1999. Clin. Chem. 45(9), 1628-1650.
Joshi, R., Janagama, H., Dwivedi, H.P., Senthil Kumar, T.M.A., Jaykus, L.-A., Schefers, J., Sreevatsan, S., 2009. Mol. Cell. Probes. 23(1), 20-28.
June, G.A., Sherrod, P.S., Hammack, T.S., Amaguana, R.M., Andrews, W.H., 1995. J AOAC Int 78(2), 375-380.
Kaerkkaeinen, R.M., Drasbek, M.R., McDowall, I., Smith, C.J., Young, N.W.G., Bonwick, G.A., 2011. Int. J. Food Sci. Technol. 46(3), 445-454.
Kariuki, J.K., McDermott, M.T., 1999. Langmuir 15(19), 6534-6540.
Karmali, M.A., 2009. Kidney Int 75, S4-S7.
Labib, M., Zamay, A.S., Kolovskaya, O.S., Reshetneva, I.T., Zamay, G.S., Kibbee, R.J., Sattar, S.A., Zamay, T.N., Berezovski, M.V., 2012. Anal. Chem. 84(21), 8966-8969.
Lazcka, O., Campo, F.J.D., Muñoz, F.X., 2007. Biosens. Bioelectron. 22(7), 1205-1217.
Liu, G., Böcking, T., Gooding, J.J., 2007. J. Electroanal. Chem. 600(2), 335-344.
Lockett, M.R., Smith, L.M., 2009. Langmuir 25(6), 3340-3343.
Ma, X., Jiang, Y., Jia, F., Yu, Y., Chen, J., Wang, Z., 2014. J. Microbiol. Methods 98, 94-98.
Malorny, B., Hoorfar, J., 2005. J. Clin. Microbiol. 43(7), 3033-3037.
Nayak, R., Kenney, P.B., Keswani, J., Ritz, C., 2003. Br. Poult. Sci. 44(2), 192-202.
Ozalp, V.C., Bilecen, K., Kavruk, M., Oktem, H.A., 2013. Future Microbiol. 8(3), 387-401.
Peterlinz, K.A., Georgiadis, R.M., Herne, T.M., Tarlov, M.J., 1997. J. Am. Chem. Soc. 119(14), 3401-3402.
Piper, D.J.E., Barbante, G.J., Brack, N., Pigram, P.J., Hogan, C.F., 2011. Langmuir 27(1), 474-480.
Polsky, R., Harper, J.C., Dirk, S.M., Arango, D.C., Wheeler, D.R., Brozik, S.M., 2007. Langmuir 23(2), 364-366.
Polsky, R., Harper, J.C., Wheeler, D.R., Dirk, S.M., Arango, D.C., Brozik, S.M., 2008. Biosens. Bioelectron. 23(6), 757-764.
Postollec, F., Falentin, H., Pavan, S., Combrisson, J., Sohier, D., 2011. Food Microbiol. 28(5), 848-861.
Radi, A.E., Montornes, J.M., O'Sullivan, C.K., 2006. J. Electroanal. Chem. 587(1), 140-147.
Revenga-Parra, M., Gómez-Anquela, C., García-Mendiola, T., Gonzalez, E., Pariente, F., Lorenzo, E., 2012. Anal. Chim. Acta 747, 84-91.
Ruffien, A., Dequaire, M., Brossier, P., 2003. Chem. Commun.(7), 912-913.
Seymour, E., Daaboul, G.G., Zhang, X., Scherr, S.M., Unlu, N.L., Connor, J.H., Unlu, M.S., 2015. Anal. Chem. 87(20), 10505-10512.
Shabani, A., Mak, A.W.H., Gerges, I., Cuccia, L.A., Lawrence, M.F., 2006. Talanta 70(3), 615-623.
Sheikhzadeh, E., Chamsaz, M., Turner, A.P.F., Jager, E.W.H., Beni, V., 2016, Biosens. Bioelectron. in press. (doi:10.1016/j.bios.2016.01.057)
Shewchuk, D.M., McDermott, M.T., 2009. Langmuir 25(8), 4556-4563.
Sivapalasingam, S., Friedman, C.R., Cohen, L., Tauxe, R.V., 2004. J. Food Prot. 67(10), 2342-2353.

Socrates, G., 2001. Infrared and Raman characteristic group frequencies : tables and charts, 3rd ed. Wiley, Chichester ; New York.
Torrens, M., Ortiz, M., Turner, A.P.F., Beni, V., O'Sullivan, C.K., 2015. Electrochem. Commun. 53, 6-10.
Torréns, M., Ortiz, M., Turner, A.P.F., Beni, V., O'Sullivan, C.K., 2015a. Electrochem. Commun. 53, 6-10.
Torréns, M., Ortiz, M., Turner, A.P.F., Beni, V., O'Sullivan, C.K., 2015b. Chem. Eur. J. 21(2), 671-681.
Torres-Chavolla, E., Alocilja, E.C., 2009a. Biosens. Bioelectron. 24(11), 3175-3182.
Torres-Chavolla, E., Alocilja, E.C., 2009b. Biosens. Bioelectron. 24(11), 3175-3182.
Vojdani, J.D., Beuchat, L.R., Tauxe, R.V., 2008. J. Food Prot. 71(2), 356-364.
Wang, J., Zhang, S., Zhang, Y., 2010. Anal. Biochem. 396(2), 304-309.
Wells, S.J., Fedorka-Cray, P.J., Dargatz, D.A., Ferris, K., Green, A., 2001. J. Food Prot. 64(1), 3-11.
Wu, W.-h., Li, M., Wang, Y., Ouyang, H.-x., Wang, L., Li, C.-x., Cao, Y.-c., Meng, Q.-h., Lu, J.-x., 2012. Nanoscale Res. Lett. 7(1), 658-658.
Yu, H.-Z., Luo, C.-Y., Sankar, C.G., Sen, D., 2003. Anal. Chem. 75(15), 3902-3907.
Zelada-Guillen, G.A., Riu, J., Duezguen, A., Rius, F.X., 2009. Angew. Chem. Int. Ed. 48(40), 7334-7337.

SCHEME AND FIGURE CAPTION:

Scheme 1. Overview of the preparation of the *Salmonella* aptasensor.

Fig. 1. Faradic complex impedance plots in 5 mM $[Fe(CN)_6]^{3-}/[Fe(CN)_6]^{4-}$ for different immobilisation steps on SPEs through electrochemical (solid line) and Zn-mediated grafting (dotted line): bare SPE (a), ACOOH/SPE (b) and Apt/ACOOH/SPE (c).

Fig. 2. Chronocoulometric response curves for modified electrodes in the absence (a) and presence of 50×10^{-6} M Ruhex via electrochemical grafting in the absence (c) and presence of aptamer (e), and Zn-mediated grafting in the absence (b) and presence of aptamer (d).

Fig. 3, (A). Bar chart of $\Delta R_{ct}/R_{ct}$ versus Log concentration of *S. typhimurium* for electrochemical and Zn-mediated grafting method **(B)**. EIS results for aptasensor incubated with different concentration of *S. typhimurium* and calibration curve for $\Delta R_{ct}/R_{ct}$ versus Log concentration of *S. typhimurium* (inset) in 5 mM $[Fe(CN)_6]^{3-}/[Fe(CN)_6]^{4-}$ in PBS buffer.

Fig. 4. Specificity of aptasensor for *S. typhimurium* detection.

Fig. 5. Curve of $\Delta R_{ct}/R_{ct}$ versus different concentration (1×10^2, 1×10^4 and 1×10^6 CFU mL^{-1}) of *S. typhimurium* in apple juice and recovery results (inset) for the detection of *S. typhimurium* from apple juice sample.

SCHEME AND FIGURES

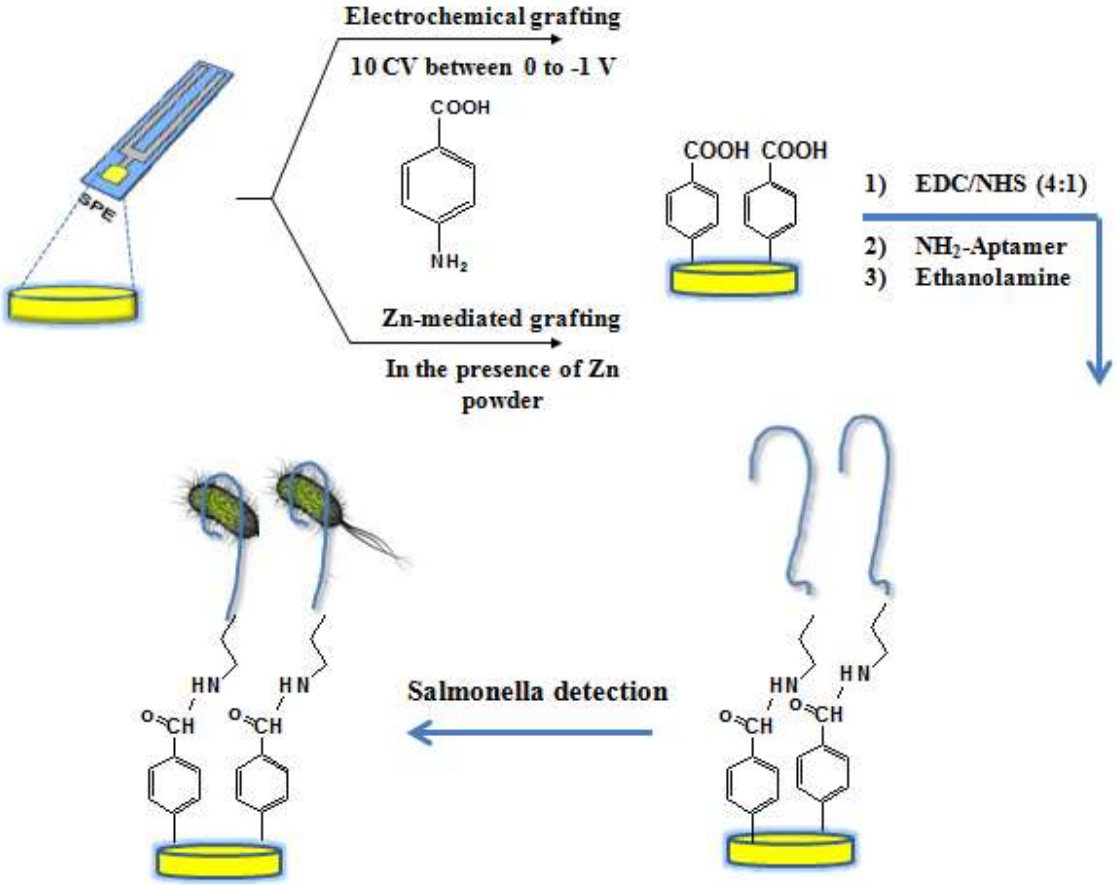

Scheme 1

529

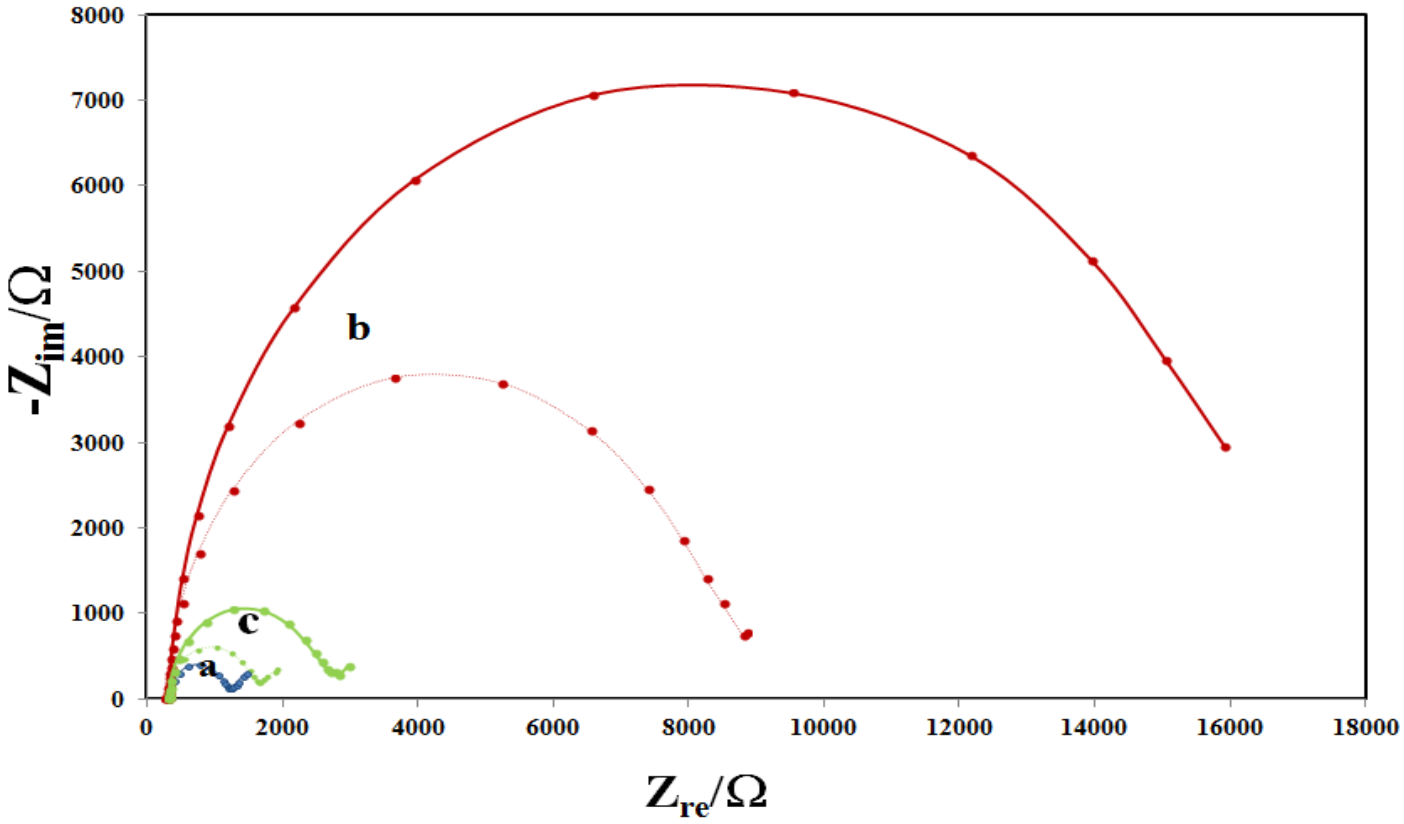

530

531 **Fig. 1**

532

533

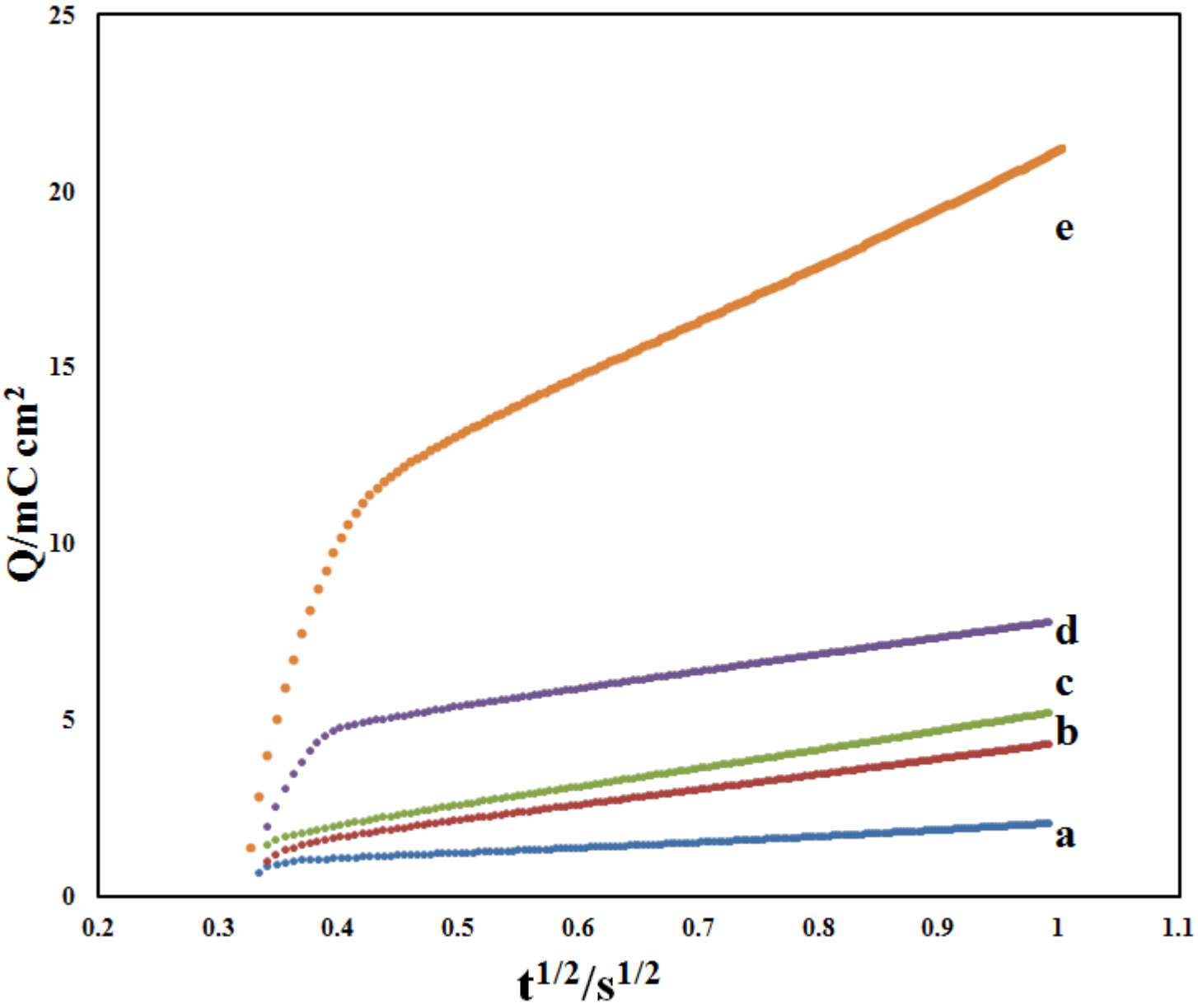

Fig. 2

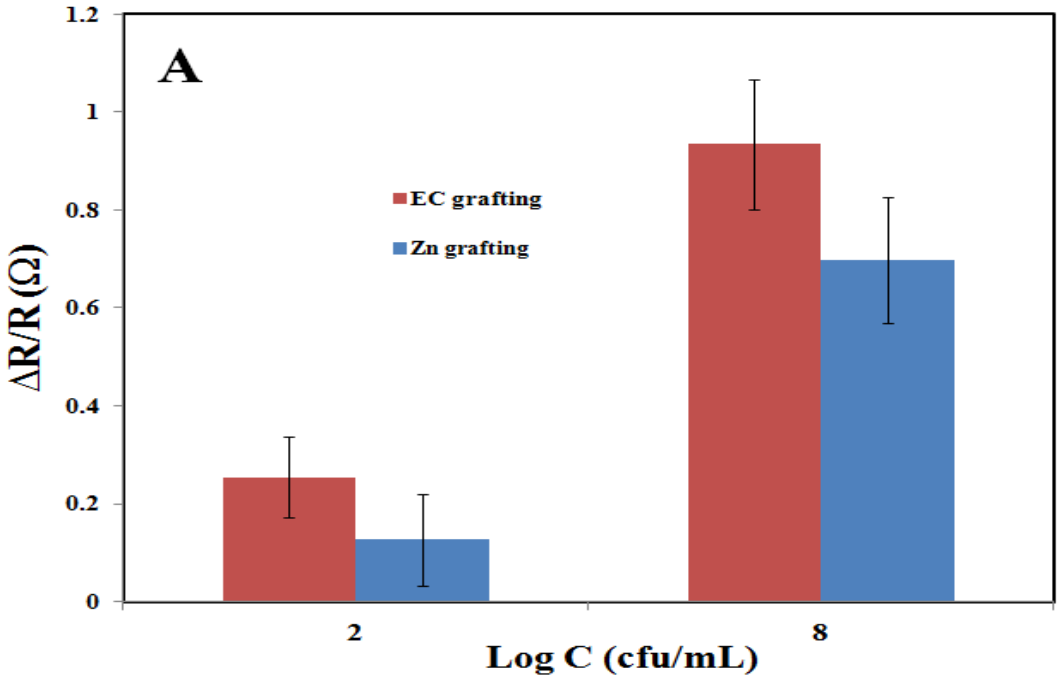

538

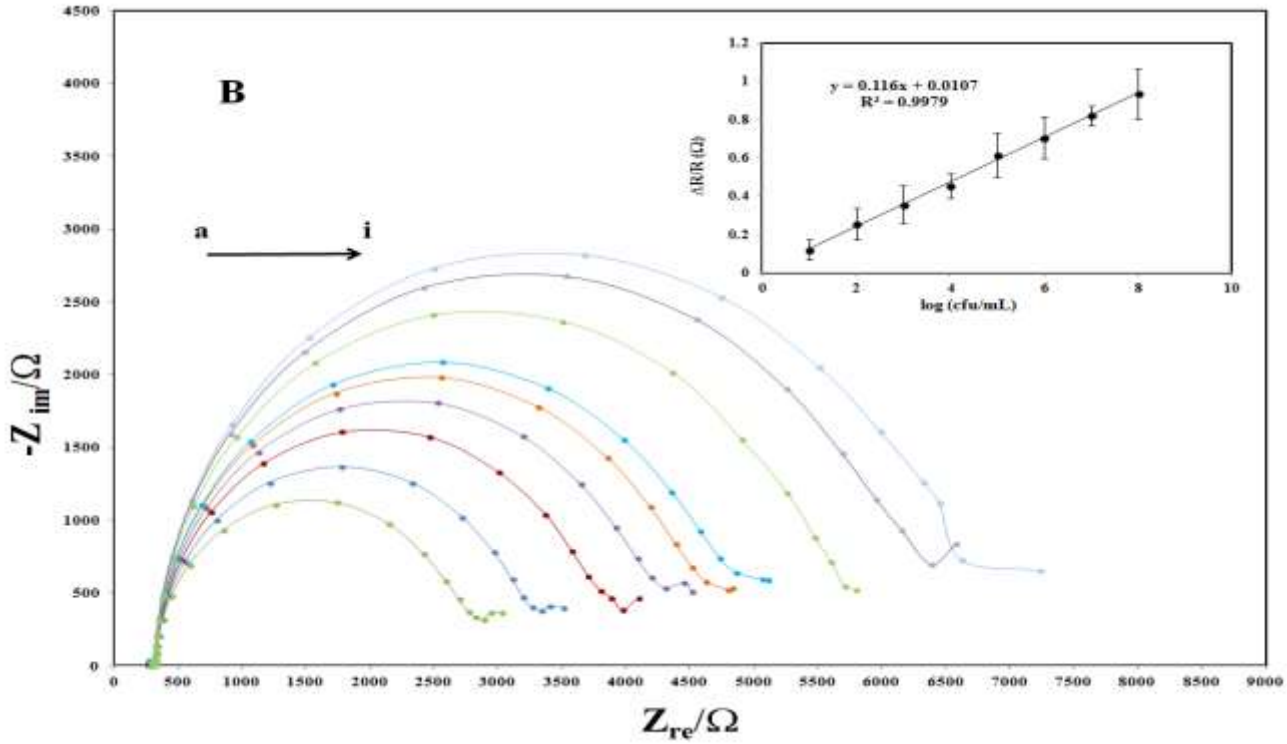

539 **Fig. 3**

540

541

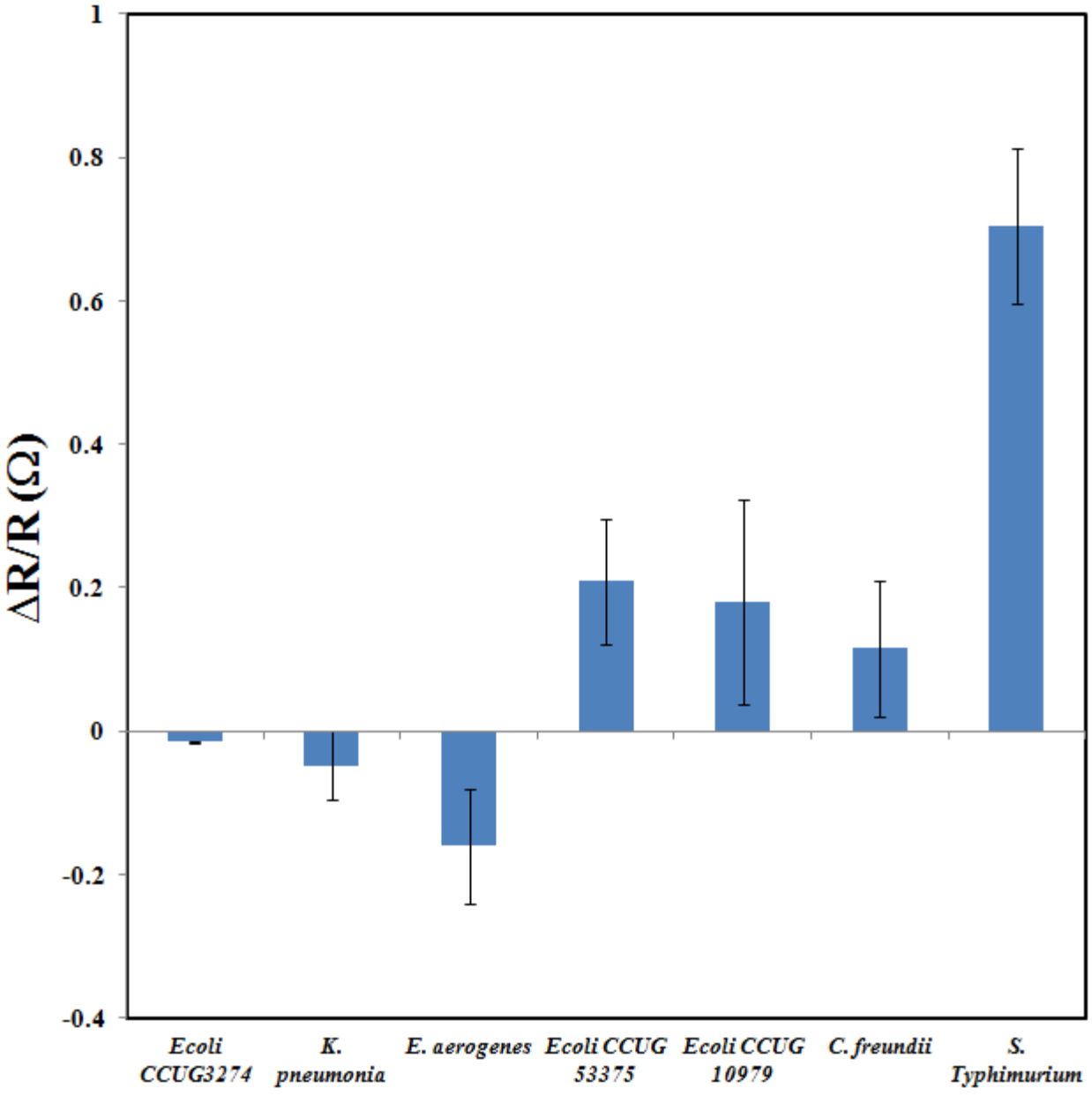

542 **Fig. 4**

543

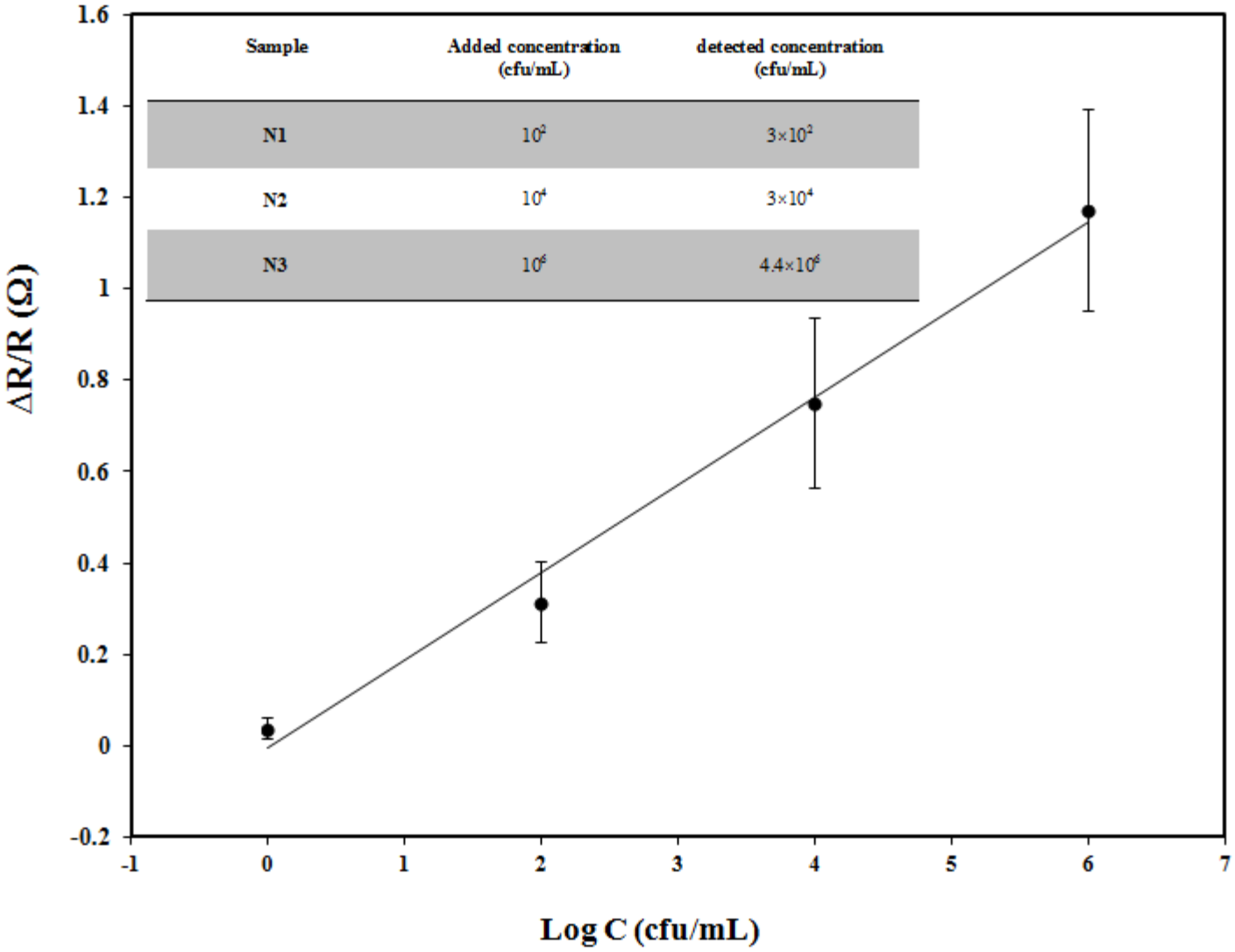

544

545

546 **Fig. 5**